Martin-Lopez, S., Abrardi, L., Corredera, P., Gonzalez-Herraez, M., Mussot, A., 2008, "Spectrally-bounded continuous-wave supercontinuum generation in a fiber with two zero-dispersion wavelengths, Optics Express, Vol. 16 , n. 9, pp. 6745-6755.

Spectrally-bounded continuous-wave supercontinuum generation in a fiber with two zero-dispersion wavelengths

Sonia Martin-Lopez[1], Laura Abrardi[1], Pedro Corredera[1], Miguel Gonzalez-Herraez[2], Arnaud Mussot[3]

[1]Instituto de Física Aplicada, CSIC. C/ Serrano, 144, Madrid 28006 Spain.
[2]Dept. of Electronics, University of Alcalá, Alcalá de Henares 28805 Spain.
[3]Laboratoire de Physique des Lasers Atomes et Molécules, Université des Sciences et Technologies de Lille, UFR de Physique, IRCICA 59655 Villeneuve d'Asq cedex, France.
E-mail: soniaml@cetef.csic.es

Abstract: A common issue in fiber-based supercontinuum (SC) generation under continuous-wave pumping is that the spectral width of the resulting source is related to the input power of the pump laser used. An increase of the input pump power leads to an increase of the spectral width obtained at the fiber output, and therefore, the average power spectral density (APSD) over the SC spectrum does not grow according to the input power. For some applications it would be desired to have a fixed spectral width in the SC and to increase the average PSD proportionally to the input pump power. In this paper we demonstrate experimentally that SC generation under continuous-wave (CW) pumping can be spectrally bounded by using a fiber with two zero-dispersion wavelengths (ZDWs). Beyond a certain pump power, the spectral width of the SC source remains fixed, and the APSD of the SC grows with the pump power. In our experiment we generate a reasonably flat, spectrally-bounded SC spanning from 1550 nm to 1700 nm. The spectral width of the source is shown to be constant between 3 and 6 W of pump power. Over this range, the increase in input power is directly translated in an increase in the output APSD. The experimental results are confirmed by numerical simulations, which also highlight the sensitivity of this configuration to variations in the fiber dispersion curve. We believe that these results open the way for tailoring the spectral width of high-APSD CW SC by adjusting the fiber dispersion.

OCIS codes: (190.4370) Nonlinear optics, fibers ; (190.4380) Nonlinear Optics, Four-wave mixing ; (190.5530) Pulse propagation and solitons ; (190.5650) Raman effect.

References and links

1. J. Dudley, G. Genty and S. Coen, "Supercontinuum generation in photonic crystal fiber," Rev. Mod. Phys. **78**, 1135 (2006), http://scitation.aip.org/getabs/servlet/GetabsServlet?prog=normal&id=RMPHAT000078000004001135000001&idtype=cvips&gifs=yes&citing=sci
2. J. K. Ranka, R. S. Windeler, and A. J. Stentz, "Visible continuum generation in air-silica microstructure optical fibers with anomalous dispersion at 800 nm," Opt. Lett. **25**, 27-27 (2000), http://www.opticsinfobase.org/abstract.cfm?URI=ol-25-1-25
3. J. M. Dudley, L. Provino, N. Grossard, H. Maillotte, R. S. Windeler, B. J. Eggleton, and S. Coen, "Supercontinuum generation in air-silica microstructured fibers with nanosecond and femtosecond pulse pumping ," J. Opt. Soc. Am. B **19**, 765-771 (2002), http://www.opticsinfobase.org/abstract.cfm?URI=josab-19-4-765
4. S. Coen, A. H. L. Chau, R. Leonhardt, J. D. Harvey, J. C. Knight, W. J. Wadsworth, and P. S. J. Russell, "Supercontinuum generation by stimulated Raman scattering and parametric four-wave mixing in photonic crystal fibers ," J. Opt. Soc. Am. B **19**, 753-764 (2002), http://www.opticsinfobase.org/abstract.cfm?URI=josab-19-4-753

5. G. Genty, M. Lehtonen, H. Ludvigsen, and M. Kaivola, "Enhanced bandwidth of supercontinuum generated in microstructured fibers," Opt. Express **12**, 3471-3480 (2004), http://www.opticsinfobase.org/abstract.cfm?URI=oe-12-15-3471
6. G. Genty, M. Lehtonen, and H. Ludvigsen, "Effect of cross-phase modulation on supercontinuum generated in microstructured fibers with sub-30 fs pulses," Opt. Express **12**, 4614-4624 (2004), http://www.opticsinfobase.org/abstract.cfm?URI=oe-12-19-4614
7. T. A. Birks, W. J. Wadsworth, and P. S. J. Russell, "Supercontinuum generation in tapered fibers," Opt. Lett. **25**, 1415-1417 (2000), http://www.opticsinfobase.org/abstract.cfm?URI=ol-25-19-1415
8. A. Mussot, T. Sylvestre, L. Provino, and H. Maillotte, "Generation of a broadband single-mode supercontinuum in a conventional dispersion-shifted fiber by use of a subnanosecond microchiplaser ," Opt. Lett. **28**, 1820-1822 (2003), http://www.opticsinfobase.org/abstract.cfm?URI=ol-28-19-1820
9. S. Kobtsev and S. Smirnov, "Modelling of high-power supercontinuum generation in highly nonlinear, dispersion shifted fibers at CW pump," Opt. Express **13**, 6912-6918 (2005), http://www.opticsinfobase.org/abstract.cfm?URI=oe-13-18-6912
10. F. Vanholsbeeck, S. Martin-Lopez, M. González-Herráez, and S. Coen, "The role of pump incoherence in continuous-wave supercontinuum generation," Opt. Express **13**, 6615-6625 (2005), http://www.opticsinfobase.org/abstract.cfm?URI=oe-13-17-6615
11. M. H. Frosz, O. Bang, and A. Bjarklev, "Soliton collision and Raman gain regimes in continuous-wave pumped supercontinuum generation," Opt. Express **14**, 9391-9407 (2006), http://www.opticsinfobase.org/abstract.cfm?URI=oe-14-20-9391
12. A. Mussot, E. Lantz, H. Maillotte, T. Sylvestre, C. Finot, and S. Pitois, "Spectral broadening of a partially coherent CW laser beam in single-mode optical fibers," Opt. Express **12**, 2838-2843 (2004), http://www.opticsinfobase.org/abstract.cfm?URI=oe-12-13-2838
13. A. K. Abeeluck, C. Headley, and C. G. Jørgensen, "High-power supercontinuum generation in highly nonlinear, dispersion-shifted fibers by use of a continuous-wave Raman fiber laser," Opt. Lett. **29**, 2163-2165 (2004), http://www.opticsinfobase.org/abstract.cfm?URI=ol-29-18-2163
14. T. Sylvestre, A. Vedadi, H. Maillotte, F. Vanholsbeeck, and S. Coen, "Supercontinuum generation using continuous-wave multiwavelength pumping and dispersion management," Opt. Lett. **31**, 2036-2038 (2006), http://www.opticsinfobase.org/abstract.cfm?URI=ol-31-13-2036
15. A. V. Avdokhin, S. V. Popov, and J. R. Taylor, "Continuous-wave, high-power, Raman continuum generation in holey fibers ," Opt. Lett. **28**, 1353-1355 (2003), http://www.opticsinfobase.org/abstract.cfm?URI=ol-28-15-1353
16. S. Martín-López, M. González-Herráez , A. Carrasco-Sanz, F. Vanholsbeeck, S. Coen, H. Fernández, J. Solís, P. Corredera and M. L. Hernanz. "Broadband spectrally flat and high power density light source for fiber sensing purposes". Measurement Science and Technology **17** 1014-1019 (2006)
17. J. C. Travers, R.E. Kennedy, S. V. Popov, J. R. Taylor, H. Sabert and B. Mangan, "Extended CW supercontinuum generation in a low water-loss holey fiber," Opt. Lett. **30**, 1938-1940 (2005) http://www.opticsinfobase.org/abstract.cfm?URI=ol-30-15-1938
18. A. Mussot, M. Beaugeois, M. Bouazaoui, and T. Sylvestre, "Tailoring CW supercontinuum generation in microstructured fibers with two-zero dispersion wavelengths," Opt. Express **15**, 11553-11563 (2007), http://www.opticsinfobase.org/abstract.cfm?URI=oe-15-18-11553
19. B. Costa, D. Mazzoni, M. Puleo, and E. Vezzoni, "Phase-shift tecnique for the measurement of chromatic dispersion in optical fibers using leds," IEEE J. Quantum Electron. **18**, 1509–1515, 1982.
20. D. Monzón-Hernández, A. N. Starodumov, Y. O. Barmenkov, I. Torres-Gómez, and F. Mendoza-Santoyo, "Continuous-wave measurement of the fiber nonlinear refractive index," Opt. Lett. 23, 1274-1276 (1998) http://www.opticsinfobase.org/abstract.cfm?URI=ol-23-16-1274
21. D. V. Skryabin, F. Luan, J. C. Knight, and P. S. J. Russell, "Soliton self-frequency shift cancellation in photonic crystal fibers," Science **301**, 1705–1708 (2003).
22. N. Akhmediev and M. Karlsson, "Cherenkov radiation emitted by solitons in optical fibers," Phys. Rev. A **51**, 2602-2607 (1995).
23. E. G. Neumann "Single-mode fibers: fundamentals" (Springer-Verlag, 1988).
24. R. H. Stolen, J. P. Gordon, W. J. Tomlinson, and H. A. Haus, "Raman response function of silica-core fibers," J. Opt. Soc. Am. B 6, 1159-1166 (1989) http://www.opticsinfobase.org/abstract.cfm?URI=josab-6-6-1159
25. O. V. Sinkin, R. Holzlöhner, J. Zweck, and C. R. Menyuk, "Optimization of the Split-Step Fourier Method in Modeling Optical-Fiber Communications Systems," J. Lightwave Technol. **21**, 61-68 (2003), http://www.opticsinfobase.org/abstract.cfm?URI=JLT-21-1-61
26. B. Barviau, S. Randoux, and P. Suret, "Spectral broadening of a multimode continuous-wave optical field propagating in the normal dispersion regime of a fiber," Opt. Lett. **31**, 1696-1698 (2006), http://www.opticsinfobase.org/abstract.cfm?URI=ol-31-11-1696
27. M. González-Herráez and L. Thevenaz. "Simultaneous position-resolved measurement of chromatic dispersion and Brillouin shift in single-mode optical fibers". IEEE Photonics Technology Letters **16** 1128-1130 (2004)

28. P. -L. Hsiung, Y. Chen, T. Ko, J. Fujimoto, C. de Matos, S. Popov, J. Taylor, and V. Gapontsev, "Optical coherence tomography using a continuous-wave, high-power, Raman continuum light source," Opt. Express 12, 5287-5295 (2004)
http://www.opticsinfobase.org/abstract.cfm?URI=oe-12-22-5287

1. Introduction

Research on supercontinuum (SC) generation in optical fibers still attracts much attention both from fundamental and applied viewpoints (See Review [1]). Up to now, wide SCs (up to two octave spanning) has been reported and have soon been considered a promising tool for metrology, biomedical and telecommunication applications, due to their high spectral brightness compared with traditional broadband light sources (incandescent or fluorescent sources). The first results were obtained with pulsed pumps [1-6] launched in Photonic Cristal Fibers (PCF), in tapered fibers [7] or in classical telecommunication fibers [8]. Except for [8], the pump wavelength was always chosen to lie close to the Zero Dispersion Wavelength (ZDW) of the fiber. For fibers exhibiting two ZDWs, the pump wavelength was normally chosen to lie between them, so as to pump in the anomalous dispersion [5,6]. It has been demonstrated that SCs generated in fibers with a single ZDW result from a complex interplay of nonlinear effects whose relative contribution depends both on the pump temporal duration and on the dispersion profile of the fiber. In PCFs showing two ZDWs, most of the studies have been performed in the femtosecond regime [5,6]. In these experimental conditions , two Dispersive Waves (DWs) could be generated because of the two ZDWs of the fiber and it was demonstrated that the SC can be bounded by these DWs.

The basic principles of SC generation in the continuous wave (CW) regime are similar to those of the pulsed regime, except that the initial CW field is first converted into a train of ultra-short pulses whose duration, peak power and temporal separation are not constant [9-12]. Since different pulses propagate in the fiber, the generation of new spectral components and the location of these new frequencies depends on the characteristics of each pulse. The overall spectrum recorded at the fiber output can be seen as the averaging of many of these individual spectra generated along the fiber. As a consequence, SCs obtained in the CW regime are usually smoother [10,13-15], and exhibit a better behaviour in terms of relative intensity noise (RIN) than those obtained in the pulsed regime [16]. From a practical point of view, recent advances in high power CW fiber lasers allow the achievement of compact and robust all-fiber SC light sources with higher Average Power Spectral Density (APSD, defined as the output power of the SC divided by its spectral width) compared with pulsed SCs [9,10,13-15]. This, of course, extends their field of application. In the first experiments, Raman fiber lasers emitting around 1500 nm were used, i.e. in the vicinity of the ZDW of dispersion-shifted fibers or some highly nonlinear fibers [10,13,14]. Due to the long fibers used, the SC extended basically to the longer wavelength part of the spectrum (compared to the pump). These spectral components are mainly due to Soliton Self Frequency Shift (SSFS) processes while the blue-shifted part of the spectrum originates from DWs [9,10]. SC extensions up to 1000 nm have been reported [10,14] with strong APSDs (10 mW/nm, i.e. 10 dBm/nm). More recently, to further increase the APSD of CW-SCs, Avdokhin et al. [15] and Travers et al. [17] have taken advantage of more powerful fiber lasers based on Ytterbium-doped fibers and of the high nonlinearity of PCFs. By the use of a low water-loss PCF, Travers *et al.* [17] achieved a SC ranging from 1100 nm to 1500 nm with an APSD of about 30 mW/nm (i.e. 15 dBm/nm).

Despite the strong APSDs reported in these references, the SC width was not controlled. Thus, increasing the pump power normally increased the SC width, but the APSD would not grow with pump power and could even be reduced (see, for instance, the evolution of the APSD with pump power in reference [14], Fig. 4). For many applications, a fixed SC width should be desirable, with a control of the PSD by means of the pump power. Recently, some

of us numerically demonstrated that by pumping a PCF showing two ZDW with a CW laser, we could achieve spectrally-bounded SC generation. In such configuration, the spectral extent of the SC would be controlled by the dispersion curve of the fiber [18], and the APSD of the SC would be controlled by the pump power (beyond a minimum input power). Using this principle, one can design a dispersion profile leading to a SC with a finite and controlled spectral extension, and tune the APSD of the source by simply changing the input pump power.

In this work we demonstrate experimentally that CW-pumped SC generation can be spectrally bounded by using a fiber with two zero dispersion wavelengths and that, in this case, the APSD can be controlled by the pump power. Additionally, this is done in the conventional telecommunication window around 1.55 μm. The core of our experiment is a flat-dispersion fiber (FDF) manufactured by Phillips and a tunable erbium-doped fiber laser (EDFL). The FDF has two ZDWs, placed at roughly 1390 and 1652 nm. Therefore, the fiber exhibits small anomalous dispersion in the region of 1500 nm, which means that it can be pumped with high-power CW EDFLs in order to obtain SC generation. Our EDFL is tunable in the range between 1545 and 1570 nm, with a maximum output power of 7 W. We show that, when a certain power is reached, the spectral extent of the supercontinuum is bounded between the pump wavelength and the longer DW, located just after the second ZDW. We confirm the validity of our results by comparing them with numerical simulations. These results are important, since they may open new ways for tailoring the spectral width of high-APSD CW SC by adjusting the fiber dispersion.

2. Experimental Setup

The experimental setup used is depicted in Fig. 1. We realized a wavelength-tunable Erbium-doped fiber ring laser delivering a maximum power of 7 W and a spectral width (FWHM) of 0.4 nm.

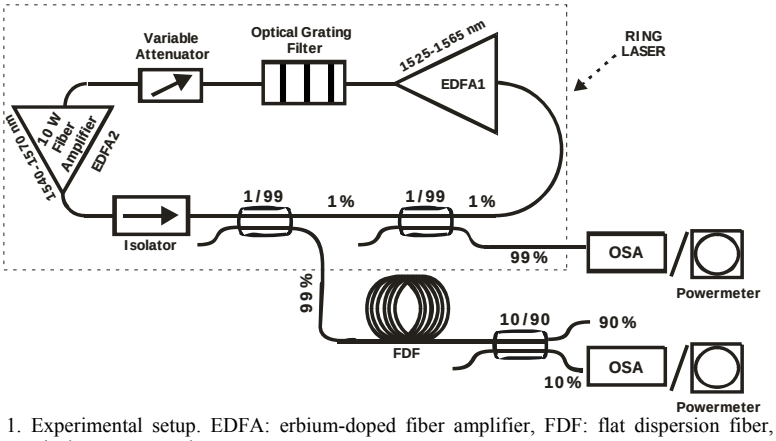

Fig. 1. Experimental setup. EDFA: erbium-doped fiber amplifier, FDF: flat dispersion fiber, OSA: optical spectrum analyzer.

As gain elements, the ring laser uses two erbium-doped fiber amplifiers (EDFAs), the first one is used just to provide a constant input power to the second one. The second one has a saturation power of nearly 10 W.

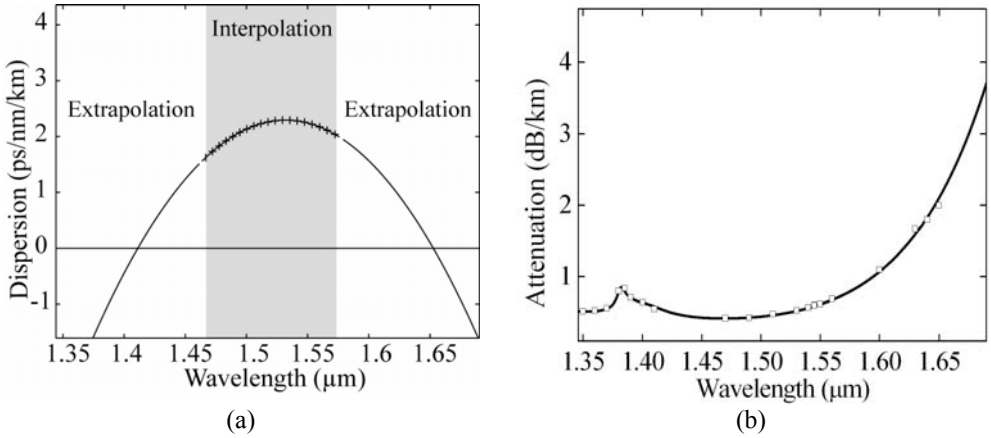

Fig. 2. (a) Dispersion curve of the 6 km FDF. The values beyond 1570 nm and under 1470 nm are extrapolated from the measured data (see text for details). (b) Measured (hollow squares) and fitted attenuation curve of the FDF.

An isolator is used after this EDFA to force the direction of the lasing and to avoid any damage in the high-power EDFA due to backreflections. The wavelength tunability of this CW source is achieved on the whole spectral band of the Erbium amplifiers by means of a tunable grating filter. Only 0.01% of the power is recirculated in the ring. This is done by means of a cascade of two calibrated 1/99 couplers. The first coupler is used to extract the biggest part of the power in the ring and launch it into the FDF. The second coupler is used to monitor the power in the ring and the spectral characteristics of the EDFL. The output spectrum is monitored by means of an Optical Spectrum Analyzer (OSA). Before the OSA, a broadband 10/90 coupler is used simply as a fixed 10 dB attenuator, to prevent damage in the OSA due to the high powers used.

The dispersion curve of the FDF has been measured between 1470 nm and 1570 nm using the phase shift method [19] (see Fig. 2(a)). By extrapolating these measurements, we obtained the first ZDW at 1410 nm and the second one at 1652 nm. Additionally, we have the plots of external measurements on these fibers done already 10 years ago. These seem to show values for the two ZDWs at 1390 nm and 1650 nm. Although it is clear that in our extrapolation the first ZDW is overestimated with respect to the external measurements of this parameter, the second ZDW seems to be consistent with the external estimations. Additionally, the rest of the curve appears nearly identical between these two limits. Considering the fact that the SC extends between the pump and the second ZDW, we believe that the most important part of the dispersion curve is the one between the pump wavelength and the the second ZDW, and not the position of the first ZDW. In our extrapolation, this part of the curve agrees very well with the external measurements, and this is why we think it can be used. Another important parameter in simulating the SC generation process is linear losses. In our case, these are particularly important in shaping the SC in the spectral region beyond 1600 nm. We measure these losses as a function of the wavelength, up to 1650 nm (see Fig. 2(b)). As remarkable features, we may point out that the maximum attenuation in the OH peak (located around 1388 nm) is roughly 0.8 dB/km, and on the longer wavelength side, the losses at 1650 nm exceed 2 dB/km. This is considerably worse than conventional fibers, probably because the confinement of the mode in the core is not as strong in this fiber as in conventional ones. We also evaluated the nonlinear coefficient of this fiber with a method based on self-phase modulation [20] and found γ=2 $W^{-1}\cdot km^{-1}$ at 1550 nm. Two samples of this fiber were used: one with a length of 6 km and the other with a length of 2 km. It must be noted that the measured dispersion profile in both samples of fiber was so close that it would be

indistinguishable in the scale of figure 2. However, as we will see in Section 4, the supercontinua generated in both samples are remarkably different. We attribute this difference to the fact that probably the dispersion profiles of the two fibers are not identical, and they actually exhibit different values of the second ZDW. Additionally, this difference is very probably reinforced by the presence of non-uniformities in the dispersion curve along the fiber. We have actually verified experimentally that the chromatic dispersion coefficient of these fibers exhibits non-uniformities along the distance, as we show in section 4.

3. Results

In this work, the spectral bounding of the SC can be assumed to be achieved by means of the same mechanisms as in the theory outlined in [18]. To summarize the theory in [18], at the beginning the MI process generates temporal spikes of a few picoseconds duration. These pulses are not stable under higher order dispersion and SRS effects and they split into quasi-fundamental solitons, leaving energy to DWs in the process. Subsequently, the SRS effect shifts these fundamental solitons towards longer wavelengths. As noted in reference [11], soliton collisions have a strong impact in enhancing the processes of splitting the initial spikes into fundamental solitons and red-shifting the fundamental solitons to longer wavelengths. Because of the special characteristics of this fiber, the frequency shift is stopped by the second ZDW. Around this wavelength, a balance is achieved between the red shift due to SRS and the blue shift due to spectral recoil when the dispersion slope of the fiber is negative [22]. The goal, therefore, is to demonstrate that SC generation under CW pumping in this kind of fibers is bounded between the pump and the second DW. The spectral position of the DWs is defined by this phase matching condition [22]:

$$\Delta\beta = \beta(\omega_P) - \beta(\omega_{DW}) = \frac{(1-f_R)\gamma(\omega_P)P_P}{2} - \sum_{n\geq 2}^{n=12} \frac{(\omega_{DW}-\omega_P)^n}{n!}\beta_n(\omega_P) = 0 \qquad (1)$$

Where $\beta(\omega_{DW})$ and $\beta(\omega_P)$ represent, respectively, the propagation constant of the dispersive wave (ω_{DW}) and the propagation component of a soliton at the angular frequency ω_P. In optical fibers having a single ZDW, the DWs are blue shifted [22] while in optical fibers with two ZDWs, two bands of DWs appear: one is blue shifted and appears below the first ZDW (λ_{01}) (DW_1); the other is red shifted and appears above the second ZDW (λ_{02}) (DW_2) [5,6].

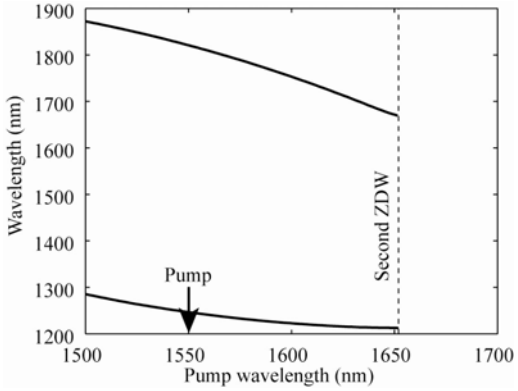

Fig. 3. Evolution of the wavelength of dispersive waves as a function of the wavelength of the soliton, as obtained from the dispersion curve represented in Fig. 2 with a pump power of 6 W .

The theoretical position of both DWs corresponding to the dispersion curve of our fiber is depicted in Fig. 3. The soliton frequency moves from the pump wavelength (1550 nm) to the vicinity of the second ZDW of the fiber (1652 nm). Under these conditions, there is two DWs that satisfy the phase-matching condition given above: one whose wavelength moves from 1250 nm to 1210 nm, and another whose wavelength moves from 1810 nm to 1680 nm. Note

that the pump power has no significant impact on the phase-matching conditions for the DWs while they are in the few watts range. The efficiency of the energy transfer from the soliton to the DWs depends on the spectral overlap between these two waves. As a consequence, even if a phase matching exists between the soliton and the DW (Eq. 1) it does not mean that a strong DW will be generated. In our case, from Fig. 4, the blue DW is very far from the pump and the spectral overlap is then negligible. The power of this DW is therefore very low, and hence the lower spectral limit of the SC is defined by the pump wavelength rather than the blue-shifted DW. As for the red-shifted DW, we should expect some power transfer to this DW due to the Raman-shifted solitons.

Fig. 4 shows the spectra measured at the output of the 6 km fiber for different input powers at a pump wavelength of 1550 nm (a), and for different wavelengths at a pump power of 7 W (b).

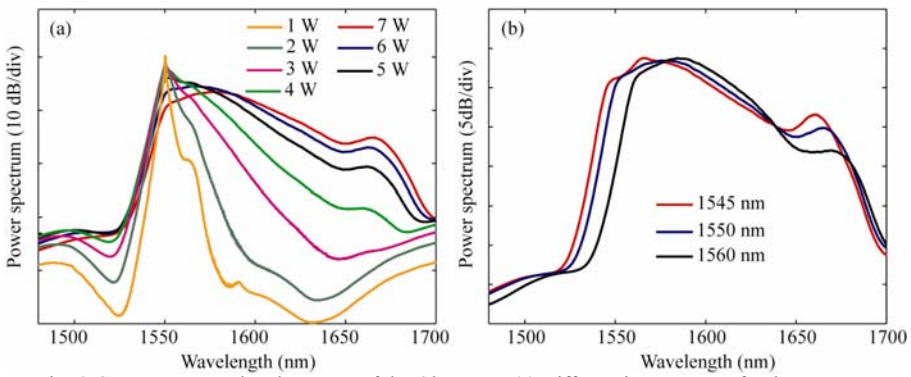

Fig. 4. Spectra measured at the output of the 6 km FDF: (a) Different input powers for the pump wavelength of 1550 nm. (b) Different pump wavelengths for a pump power of 7 W.

As it was expected, the spectral bounding of the SC is achieved in this fiber between the pump wavelength at 1550 nm and the second DW generated at about 1675 nm. This DW should be caused by solitons which are shifted just below the second ZDW (Fig. 3). As it can be seen, the limits of the SC remain constant from 4 W up to 7 W. The position of the second DW did not depend on the pump power, in good agreement with the reasoning given above. As a consequence, for a fixed pump wavelength we were able to control the APSD of the SC by simply tuning the pump power. For instance, pumping at 1550 nm, an increase in the input pump power from 4 to 7 W led to a raise in the APSD of the SC from 0.96 dBm/nm to 1.87 dBm/nm. It must be noted that the increase in APSD is not proportional to the pump power. This is probably due to the fact that the losses in the fiber are strongly wavelength-dependent (they are higher for longer wavelengths). When the pump power is increased, the longer-wavelength part of the SC is being enhanced. The frequencies lying in this part of the spectrum experience more losses than the wavelengths lying closer to 1550 nm.

In Fig. 4(b), the output spectra obtained at three different pump wavelengths are represented. The upper limit of the SC remains nearly constant, even if we observed a slight modification of the position of the peak around 1670 nm. It is difficult to determine if this peak is mainly due to the SRS effect (the spectral shift from the pump is around the SRS shift, 106 nm at 1550 nm) or to the second DW whose location is also predicted around this wavelength (Fig. 3).

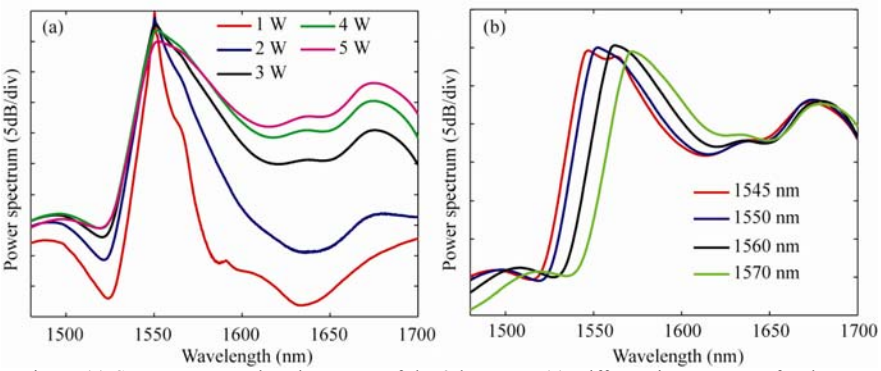

Fig. 5. (a) Spectra measured at the output of the 2 km FDF: (a) Different input powers for the pump wavelength of 1550 nm. (b) Different pump wavelengths for a pump power of 5 W.

Numerical simulations of the SC generation process in the 2 km fiber (see Section 4) show that the steady-state behaviour is reached from around 1 km, and beyond that length, no improvement in the SC characteristics is obtained. Thus, from a practical point of view, a shortening of the fiber would lead to an increase of the APSD. This is why we realized the same experiments in the 2 km long FDF.

In Fig. 5(a) we can see that, as the pump power grows, the spectral broadening is greater and for powers beyond 2-3 W the SC seems to stop just above 1700 nm. Of course we can not know if there is any further peak beyond 1700 nm since unfortunately this is the upper limit of our optical spectrum analyzer. One may think that the broad peak located around 1660 nm is due to Stimulated Raman Scattering caused by the pump. However, we can see in Fig. 5(b) that its position does not change exactly in the same amount as the pump wavelength, as it would be the case of SRS (a 10 nm shift in the pump at 1550 nm should be translated into an 11.6 nm shift in the Raman peak, corresponding to 13.2 THz of frequency shift). The wavelength variation of the peak with the pump wavelength in this case seems to correspond to that of a pure DW. If this is truly a DW, the SC spectrum should be bounded by the DW, and no power beyond 1700 nm should be expected. Numerical simulations are performed in the next section to get a clearer insight on this phenomenon.

As a conclusion of this part, we can say that we have experimentally demonstrated that CW SC generation can be spectrally bounded in a fiber with two ZDWs. Moreover, we also demonstrated that from a certain pump power, the APSD can be controlled by tuning the pump power. It is important to point out that this behavior is very different from that of a fiber with a single ZDW, where an increase of the pump power leads to an increase of the broadening and not of the APSD.

4. Numerical simulations

We modeled the propagation of the CW field using the generalized nonlinear Schrödinger equation (NLSE) [1]:

$$\frac{\partial E}{\partial z} = i\sum_{m\geq 2}^{m=12}\frac{i^m \beta_m}{m!}\frac{\partial^m E}{\partial \tau^m} + i\gamma(\omega_0)\left[1+\frac{i}{\omega_0}\frac{\partial}{\partial \tau}\right]\times\left[E(z,\tau)\int_{-\infty}^{+\infty}R(\tau')\left|E(z,\tau-\tau')\right|^2 d\tau'\right] - \frac{\alpha(\omega)}{2}E \quad (2)$$

Where $E(z,\tau)$ is the electric field envelope in a retarded time frame $\tau=t-\beta_1 z$ moving at the group velocity $1/\beta_1$ of the pump. ω_0 is the carrier angular frequency of the CW input field and $\gamma(\omega_0)$ is the nonlinear coefficient at the pump wavelength (2 $W^{-1}\cdot km^{-1}$ @ 1550 nm). The

dispersion parameters β_m are estimated from a polynomial fit of order 12 to reach a good interpolation of the fiber dispersion profile (Fig. 2). $\alpha(\omega)$ is the linear losses of the FDF. For the linear losses of the fiber, we take a fairly standard model of the spectral attenuation of the fiber [23] and we fit the parameters to get an attenuation curve that matches our measurements in the relevant points (OH peak at 1390 nm and losses at 1650 nm).. Dispersion effects are described by the first term on the right hand side of Eq. (2) while nonlinear optical effects such as Self-Phase Modulation, SRS, self-steepening and shock-wave formation correspond to the second one. $R(\tau)=(1-f_R)\delta(\tau)+ f_R x h_R(\tau)$ is the nonlinear response of silica (f_R=0.18), where we used the experimentally measured Raman response of silica fibers for $h_R(\tau)$ [24]. The convolution integral in Eq. (2) between the field intensity and the delayed Raman response is calculated as a simple product in the frequency domain. Both real and imaginary parts of the Raman susceptibility are included. The time derivative term of the self-steepening effect is numerically calculated in the frequency domain. Equation 2 is solved numerically using the adaptive step size method outlined by Sinkin *et al.* [25] since it reduces the total number of Fourier transforms and thus increases computation speed. The local goal error used in the adaptive step size method was set to $\delta_G=10^{-4}$. It corresponds to a good trade off between accuracy and computation speed. The number of points in the simulation was 65536 and the temporal and spectral windows were, respectively, 0.33 ns and 200 THz. These figures lead to a frequency step of 3 GHz and a time step of 5 fs. We have verified that the photon number is preserved in our simulation within 1%, and we have verified that the step size we choose is adequate since reducing the local goal error to 10^{-3} gives comparable results.

An important issue in this simulation is how to model the partial coherence of the fiber laser used. In these simulations we used the experimental power spectrum of the laser with a random spectral phase on each longitudinal mode [10,27]. There are three key reasons to use this "phenomenological" model: first, high-power fiber lasers exhibit fast intensity instabilities on the time scale of the coherence of the source, as shown by autocorrelation measurements in reference [10]. This random succession of picosecond pulses (about the inverse of the full width half maximum of the pump) are well reproduced with this "phenomenological" model, but are not taken into consideration in a simple phase diffusion model. It may be argued that a cw signal with phase noise propagating in a dispersive fiber will actually develop intensity noise after some distance. However, it must be stressed that intensity instabilities have been observed at the output of fiber lasers, and not only after propagation in dispersive fibers. Second, to generate a perfectly continuous wave in the time domain all the longitudinal modes of the fiber laser have to be specially phase matched. This condition seems extremely difficult to achieve in fiber lasers, which usually have long cavity lengths (this one too). Third, our experience is that this model leads to the best agreement between experimental and numerical results in the case of supercontinuum. A discussion on the validity of this model can be found in Refs [11,18], but up to date and to our knowledge, this is the best way to reproduce the experimental behavior of these light sources.

We tried to reproduce in our simulations the results in the 2 km fiber. We performed our simulation with 6 W of pump power launched at 1550 nm. It must be stressed that the measured losses of the fiber have been included in the numerical simulations. The results obtained can be seen in Fig. 6(b), red trace. The experimental results are also shown for comparison (dashed line). We can see a moderate agreement between the numerical and experimental results: in both cases there is no power below the pump wavelength, and also in both cases there appears a maximum in the spectrum lying beyond the second ZDW, which is attributed to DW generation. The position of this maximum, however, is different in both cases, and the simulated spectrum appears to be more extended than the experimental one. We consider that this difference may be due to errors in our determination of the second ZDW. Since the measurements of the dispersion curve have only been performed between 1470 nm and 1570 nm, the rest of the curve has been extrapolated. This should lead to errors in the determination of the second ZDW, leading to strong changes in the expected position of the

DWs. To illustrate more clearly this issue, we simulated the SC obtained with three identical fibers except for their dispersion curves, which are slightly different. Fig. 6(a) shows the three simulated dispersion curves (the red one is the dispersion curve of Fig. 3, so the one inferred from the measurements), while Fig 6(b) shows the corresponding spectra obtained at the fiber output.

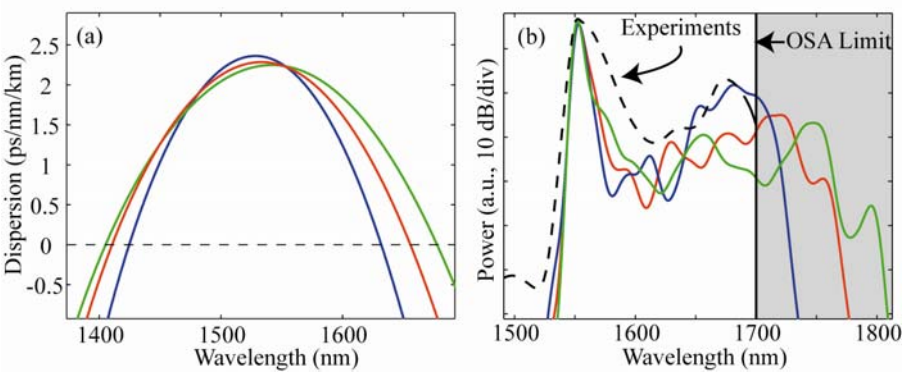

Fig. 6. (a) Three slightly different dispersion curves for the FDF and (b) corresponding output spectra at the output of the 2 km fiber for 6 W and λ_P=1550 nm. The dotted line represents experimental results.

We can see the extreme sensitivity of the output spectrum to small dispersion changes. In particular, the position and height of the second DW is strongly dependent on the position of the second ZDW. We notice that the measured spectrum is extremely similar to one of the simulated ones (blue line).

It must be mentioned that the spectra obtained in Fig 6(b) have been done using only one simulation and the smoothing technique used in [18]. Due to the stochastic nature of the model used to simulate the CW pump, one has usually to performed tens of simulations to realize an averaging in order to get a realistic spectrum directly comparable with the experimental one [10,26]. However, as it was demonstrated in Ref. [18], in a fiber with two ZDWs it is not necessary if the fiber length is long enough. In this case, the soliton is stopped just below the second ZDW and the global shape of the SC is not further modified by propagating inside the fiber. A similar reasoning applies for the different temporal profiles used at the input of the simulation. Once the spectral broadening of the pump has reached the second ZDW and the second DW is generated, the change of the shape of the SC is not significant [18]. This is verified in Fig. 7-(a), where 4 successive simulations are performed with the blue dispersion curve of figure 6(a). As it can be seen, the difference among successive simulations is largely negligible. Note that the spectrum has been smoothed by using the method described in Ref. [18] to get a clearer figure. One example of smoothing is represented in Fig. 7-(b). The input temporal profile of the pump in each simulation is represented in Fig. 7-(c).

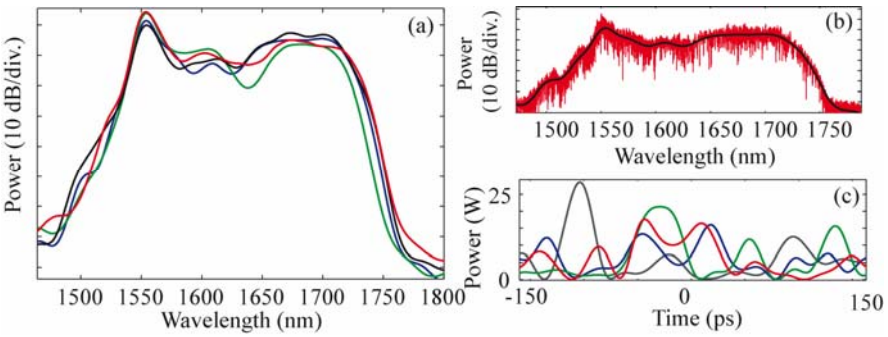

Figure 7 : (a) four successive simulations with the blue dispersion curve of figure 6. (b) example of smoothing to get a clearer figure. (c) temporal input intensity of the pump wave.

Considering this, one may wonder why there is so much difference between the experimental spectra obtained in the 2 and the 6 km fiber. If the shape of the SC is preserved once the steady state is reached, the spectra in the 2 km and the 6 km fiber should be nearly identical (except for the mean power) since they have the same overall dispersive properties. We believe that this difference is due to longitudinal fluctuations of the dispersion. Some measurements in standard telecommunication fibers [27] have shown that these variations of dispersion can be extremely important, specially if we consider that the fiber is relatively old and unconventional. To confirm it, we measured the dispersion in two pieces of 100 m at each end of the 6 km fiber with a pulsed laser at 1550 nm by looking at the location of MI side lobes. In one piece, we found a value for the dispersion coefficient of D=0.5 ps/nm/km at 1550 nm. In the other piece, we can not see the characteristic MI side lobes, thus indicating that the dispersion coefficient is negative (D<0). Dispersion variations should completely destroy the phase-matching conditions and drastically reduce the efficiency of the power transfer between the solitons and the DWs. This effect should be more relevant when the involved spectral components lie far away from each other and the fiber is long, as it is the case in the 6 km fiber.

5. Conclusion

In this paper, for the first time to our knowledge, we have experimentally demonstrated that SC generation under CW pumping can be spectrally bounded by using a fiber with two ZDWs. We achieved a quite flat SC spanning from 1550 nm to 1700 nm. The APSD in the fiber could be tuned in the range of several mW/nm. It is worth noting that all the pump power has been converted into the SC, leading to a good figure of merit compared with previously reported CW SC results. This experimental result has been confirmed by numerical simulations and opens the way for tailoring the spectral width of high-APSD CW SC sources by adjusting the fiber dispersion. These sources would be of primary interest for optical coherence tomography applications [28].

Acknowledgments

We acknowledge financial support from the Ministerio de Educacion y Ciencia through projects TEC2006-09990-C02-01 and TEC2006-09990-C02-02, the support from CSIC through project MeDIOMURO, the support from the Comunidad Autónoma de Madrid through the projects FUTURSEN S-0505/AMB/000374 and FACTOTEM S-505/ESP/000417, the support from Social European Fund through the grant program I3P of CSIC and the COST Action 299 “FIDES”. IRCICA and CERLA are supported by the “Conseil regional du nord pas de Calais” and “the fond européen du développement économique des regions”.